

# Subharmonics in photorefractive crystals

A. Blendovski, J. Otten, K. H. Ringhofer, and B. Sturman

*Institute for Automation and Electrometry, Siberian Div., Russian Academy of Sciences*

(Submitted 20 January 1992)

Zh. Eksp. Teor. Fiz. **102**, 406–423 (August 1992)

We show that the dielectric grating induced by an external probe in a photorefractive crystal with the period of the external probe can be unstable against period multiplication. We investigate analytically and numerically the conditions for the excitation of the resulting spatial subharmonics and their properties, and explain the basic behavior observed in experiment.

## INTRODUCTION

The primary source of the giant optical nonlinearities exhibited by photorefractive crystals (PRC) such as  $\text{LiNbO}_3$ ,  $\text{BaTiO}_3$ , and BSO is the creation by two waves with wavenumbers  $\mathbf{k}_1$  and  $\mathbf{k}_2$  of a refractive index grating with period given by the difference vector  $\mathbf{K} = \mathbf{k}_1 - \mathbf{k}_2$ , as shown in Fig. 1. The change in index of refraction of a PRC is linearly related to the electrostatic field  $\mathbf{E}(\mathbf{r})$  arising from charge separation under the action of light. The frequencies of the optical wave are so close that their difference has no effect on the common magnitude of the wave vectors  $\mathbf{k}_{1,2}$ .

Many important nonlinear-optics effects are associated with the creation of a refractive index grating and Bragg diffraction by this grating: amplification and correction of weak optical beams,<sup>1,2</sup> phase conjugation,<sup>3,4</sup> photo-induced scattering,<sup>4,5</sup> etc. In PRC effects connected with the higher space harmonics  $2K$ ,  $3K$ , ... are also well known.<sup>6,7</sup> Such gratings form because of the nonlinearity of the constitutive equations which describe the charge separation.

In 1988, Mallick *et al.*<sup>8</sup> conducted experiments on BSO crystals in which they observed the spontaneous appearance of additional optical beams, which corresponded to diffraction of the pump waves by gratings with fractional spatial frequencies  $K/2$ ,  $K/3$ , and  $K/4$  (see Fig. 1). The experiments were carried out in the presence of an external field  $E_0 = 8 \text{ kV/cm}$  and a frequency detuning  $\Omega$  on the order of 10 Hz. The angle between the pump beams was small enough that these authors observed not only the process of mutual Bragg diffraction of the waves  $\mathbf{k}_{1,2}$  by the grating  $\mathbf{K}$ , but also scattering of the pump waves by gratings with vectors  $c\mathbf{K}$  ( $c \leq 1$ ), i.e., ultra-Bragg diffraction. A characteristic of these experiments is that as the detuning  $\Omega$  increases there first appear additional waves that correspond to the first subharmonic ( $K/2$ ), followed by second ( $K/3$ ), and third ( $K/4$ ) subharmonic waves. The optical beams that appear have small angular divergence, comparable to the divergence of the pump beams. In Refs. 9–12 many of the results of Ref. 8 were confirmed, and a number of additional data were obtained that added detail to the picture of the effect.

Several attempts were made to explain the data observed. In Refs. 13–15 the appearance of spatial subharmonics was associated with "optical" instability of the two-beam configuration. In other works, model relations were used for the nonlinear response (corresponding only to gratings at the spatial difference frequencies of the waves), while the fact of the instability was associated with the structure of the equations for the optical wave amplitudes. However, this approach does not allow one to give even a qualitative expla-

nation of the fundamental experimental regularities. In Ref. 16 the hypothesis was advanced that the observed effects were a consequence of instability of a PRC located in the field of two optical waves  $\mathbf{k}_{1,2}$  relative to the generation of spatial subharmonics of the electric field at  $K/2$ ,  $K/3$ ,  $K/4$ . This assumption goes beyond the boundaries of traditional descriptions of PRC nonlinearity, and is a photoelectric phenomenon new to physics.<sup>1)</sup> Confirmation of the hypothesis given above was provided by the authors of Refs. 10 and 16, whose numerical data indicated amplification at the first subharmonic  $K/2$ .

In this paper we propose a first-principles theory of these PRC spatial subharmonics based on a combination of analytical and numerical results. Some of the results we present here were previously published in Ref. 20, while several analytical results applying specifically to the first subharmonic  $K/2$  were published independently in Ref. 21.

The article is structured as follows: in Ref. 1 we present the basic equations for the space charge field, introduce dimensionless variables, and discuss possible simplifications. Those properties of a grating without subharmonics that are required for further discussions are discussed in Sec. 2. In Sec. 3 we use an elementary mechanical analogy to demonstrate that strongly nonlinear steady-state subharmonic solutions are possible, and investigate the coarse structure of the subharmonic branches. In Sec. 4 we obtain simple analytical expressions for the  $1/2$  and  $1/3$  steady-state subharmonics. In Sec. 5 we show that a grating without subharmonics is unstable against the creation of new spatial frequencies. In Sec. 6, we analyze the conditions for realization of the subharmonic regime in terms of the fundamental characteristics of the PRC and the experimental parameters. It is here that we compare the theory and the basic experimental results. Results of numerical modeling, presented in Sec. 7, show good agreement with the analytical theory and

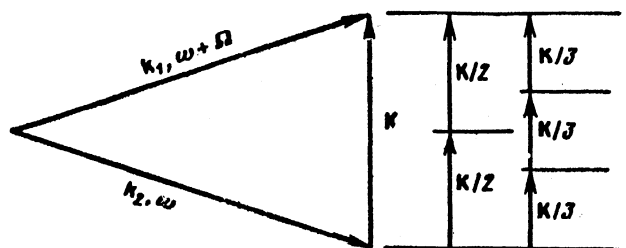


FIG. 1. Descriptive sketch of the grating and subharmonic generation process.

illustrate how the steady-state subharmonic regime is established, along with some nontrivial properties of the transient processes. In conclusion we summarize the fundamental results of the paper and indicate prospects for further investigations.

## 1. FUNDAMENTAL EQUATIONS

In order to describe the photoinduced field  $\mathbf{E}(\mathbf{r}, t)$  we must augment the equations of electrostatics and continuity

$$\operatorname{div} \mathbf{E} = \frac{4\pi\rho}{\bar{\epsilon}}, \quad \frac{\partial\rho}{\partial t} + \operatorname{div} \mathbf{j} = 0, \quad (1)$$

where  $\bar{\epsilon}$  is the dielectric permittivity, with model relations for the charge density  $\rho$  and the electric current  $\mathbf{j}$ . In the simplest and most widely used PRC models, the density  $\rho$  is represented by contributions from free electrons, ionized active centers (donors), and compensating centers (acceptors), while the current is associated with diffusion and drift of free carriers. The relations for  $\mathbf{j}$  and  $\rho$  that correspond to this model have the form<sup>1</sup>

$$\mathbf{j} = q\mu n\mathbf{E} + \mu T \nabla n, \quad \rho = q(N_D^+ - N_A - n), \quad (2)$$

$$\partial N_D^+ / \partial t = s_i I (N_D - N_D^+) - s_r n N_D^+,$$

where  $q$  is the absolute value of the electron charge,  $\mu$  is the mobility,  $n(\mathbf{r}, t)$  is the number density of free carriers,  $T$  is the temperature in energy units,  $N_D^+(\mathbf{r}, t)$  is the density of ionized donors,  $N_D$  is the total donor density,  $N_A$  is the density of compensating acceptor centers,  $I(\mathbf{r}, t)$  is the light intensity, and  $s_{i,r}$  are the ionization and recombination rates. In (2) we neglect thermal excitation of electrons; usually this approximation is applicable for PRC even for very small light intensities. The constancy of the external field  $\mathbf{E}_0$  and the neutrality of the crystal are expressed through obvious relations for the spatial averages:

$$\bar{\mathbf{E}} = \mathbf{E}_0, \quad \bar{N}_D^+ - \bar{n} = N_A. \quad (3)$$

In the absence of illumination we have  $N_D^+ = N_A$ . The constants  $s_{i,r}$  can be related to the absorption coefficient of the crystal  $\alpha$  and the lifetime of a photoelectron  $\tau$ :

$$s_i(N_D - N_A) = \alpha / \hbar\omega, \quad s_r N_A = \tau^{-1}, \quad (4)$$

where  $\hbar\omega$  is the energy of the incident photons.

In accordance with the primary scheme illustrated in Fig. 1, we choose the light intensity in the form of a traveling grating:

$$I = I_0 [1 + m \cos(\mathbf{K}\mathbf{r} - \Omega t)],$$

$$I_0 = I_1 + I_2, \quad m = 2(I_1 I_2)^{1/2} / I_0. \quad (5)$$

The parameter  $m$ , which depends on the ratio of the intensities of the pump waves  $I_{1,2}$  characterizes the modulation depth of the grating. The case of uniform illumination corresponds to  $m = 0$ ,  $E = E_0$ ,  $n = \bar{n}$ . In the region of not-too-great intensities, i.e., when  $\bar{n} \ll N_D^+ \approx N_A$ , we have  $\bar{n} = n_0 = \alpha I_0 \tau / \hbar\omega$ .

Let us now simplify the original system of equations (1) and (2). We will make use of the usual adiabatic approximation for the density of free electrons, neglecting  $\partial n / \partial t$  in comparison with  $n / \tau$ . The conditions for this approximation are that the lifetime  $\tau$  be small compared to the remaining characteristic times (in particular compared to  $\Omega^{-1}$ ). If we

limit ourselves to the region of not-too-large intensities (when  $n \propto I$ ), we may also neglect contributions from free carriers to the space charge density for  $E$ . The conditions under which these approximations are valid, which are fulfilled quite well in the majority of experiments on PRC, are specified in Secs. 2 and 5. A second general assumption will be that the problem be one-dimensional; i.e., all quantities are assumed to depend only on a single space variable  $\mathbf{K}\mathbf{r}$  (in this case we obviously have  $\mathbf{E} \parallel \mathbf{K}$ ).

We now transform from  $n, E, N_D^+$  to the dimensionless variables  $p, e, u$ , and from  $\mathbf{K}, \mathbf{r}$ , and  $t$  to the dimensionless coordinates  $x'$  and  $t'$ :

$$p = \frac{n}{n_0}, \quad e = \frac{E}{E_0}, \quad u = \frac{N_A - N_D^+}{N_D - N_A},$$

$$x' = \mathbf{K}\mathbf{r} - \Omega t, \quad t' = s_i I_0 t. \quad (6)$$

As a result, the system of equations (1) and (2) takes the form

$$u_{t'} - \Delta u_{x'} = p(1 - \eta u) - f(1 + u), \quad (7)$$

$$p(1 - \eta u) - f(1 + u) = K l_0 (pe)_{x'} - K^2 l_D^2 p_{x'x'},$$

$$e_{x'} = -\beta u.$$

Here  $\Delta = \Omega / s_i I_0$  is the dimensionless detuning,  $\eta = (N_D - N_A) N_A^{-1}$ ,  $l_0 = \mu \tau E_0$  is the drift length,  $l_D = (\mu \tau T / q)^{1/2}$  is the electron diffusion length,  $\beta = 4\pi q (N_D - N_A) K \bar{\epsilon} E_0$ , and the subscripts  $x'$  and  $t'$  denote differentiation. The dimensionless function  $f(x')$  gives the spatial intensity modulation

$$f = 1 + m \cos x'. \quad (8)$$

The parameter  $\eta$  characterizes the degree of compensation of the crystal: for  $\eta \gg 1$ , most of the donor centers are occupied by electrons. In place of condition (3), we now have  $\bar{e} = 1$ ,  $\bar{u} = 1$  for the dimensionless averages.

Despite our simplification of Eqs. (7), the latter are too complicated to be solved in closed form. Our analytical approach will consist of the following procedure: we first identify which independent contributions to (7) are responsible for the appearance of subharmonics, and which ones impede their appearance. We then discard the "harmful" independent terms, and reduce (7) to a simplified system of equations which we investigate in detail. We then develop a perturbation theory with respect to the "harmful" terms, calculating the degree to which they influence the subharmonics and the conditions under which we can neglect them.

Let us first assume that the instability of the PRC against subharmonics is connected with the drift nonlinearity, i.e., with the term  $(pe)_{x'}$  in (7), and at the same time classify reoccupation of traps and diffusion of photoelectrons as "harmful" effects. Neglecting the quantities  $u$  and  $\eta u$  compared with unity, and discarding the diffusion term  $p_{x'x'}$ , we are led to the simplified system of equations

$$u_{t'} - \Delta u_{x'} = p - f,$$

$$p - f = K l_0 (pe)_{x'},$$

$$e_{x'} = -\beta u. \quad (9)$$

From (9) it follows immediately that  $\bar{p} = 1$ . For the steady-state solution of (9) we have

$$e(e_{x'x'} + \epsilon f) - v_E e_{x'} = \epsilon c, \quad (10)$$

where  $\varepsilon$  and  $\nu_E$  are two important dimensionless parameters,

$$\varepsilon = \beta/\Delta, \quad \nu_E = (Kl_0)^{-1}, \quad (11)$$

and  $c$  is an integration constant which should be determined from the solution to Eq. (10) and the condition  $\bar{x} = 1$ .

From a formal point of view, the steady-state equation (10) can be viewed as an equation of motion for a particle of unit mass placed in a potential field and subjected to the action of a force that is periodic in "time." The amplitude of this driving force is  $\varepsilon m$ , and the shape of the potential is related self-consistently to the characteristics of the motion. The parameter  $\nu_E$  has the sense of a friction coefficient. As we will see below,  $\varepsilon$  is the fundamental parameter that determines the appearance of subharmonics.

With regard to this mechanical analogy, we note that the behavior of a nonlinear oscillator under the action of an external periodic force, which is described in great detail in the literature,<sup>17,18</sup> is characterized by a variety of subharmonic solutions. However, a direct analogy between (10) and the equations under study here is not possible.

## 2. STEADY-STATE SOLUTION WITHOUT SUBHARMONICS

It is completely obvious that both the original equations (7) and the simplified system (9) have solutions that do not contain subharmonics, and can be written in the form of a Fourier series

$$e(x', t') - 1 = \sum_{n=1}^{\infty} e_n(t') \exp(inx') + c.c. \quad (12)$$

Similar expansions are valid for  $p$  and  $u$ .

In those cases where the amplitude of the periodic external force  $\varepsilon m$  is sufficiently small, we can expect rapid convergence of the series (12). Using an iterative procedure, it is not difficult to obtain from (7) the following expressions under steady-state conditions:

$$e_1 = \frac{\varepsilon m}{2(1 - \varepsilon + i\gamma_1)}, \quad \gamma_1 = \nu_N + \varepsilon(\nu_E + \nu_D), \quad (13)$$

where

$$\nu_N = (1 + \eta)/\Delta, \quad \nu_D = KT/qE_0. \quad (14)$$

Based on its structure, Eq. (13) is analogous to the expression for the amplitude of forced vibrations of an oscillator with characteristic frequency  $\sqrt{\varepsilon}$  and attenuation  $\gamma_1$ . It is clear that the diffusion of carriers and reoccupation of traps leads only to renormalization of the parameter  $\gamma_1$ . Within the framework of the simplified Eq. (10),  $\gamma_1 = \varepsilon\nu_E$ . Equation (13) is valid for  $\varepsilon \lesssim 0.3$  to  $0.4$ , and  $\gamma_1 \ll 1$ ;  $\varepsilon$ -dependent corrections to this expression begin with terms of order  $\varepsilon^4$ .

The second harmonic of the field  $e_2$ , in which we neglect the parameters  $\nu_{E,D,N}$ , has the form  $e_2 \approx -m^2\varepsilon^3/16$ ; it is obvious that  $|e_2| \ll |e_1|$ .

We note that the search for a steady-state solution  $e(x')$  in the form of a series in powers of  $\varepsilon$  leads only to a solution that does not contain subharmonics. This indicates that the subharmonic steady states is associated with a bifurcation of the solution, and can only exist starting with finite values of  $\varepsilon$ .

## 3. MECHANICAL ANALOGY

Using the direct mechanical analogy described above, it turns out to be possible to identify a number of nontrivial and general properties of the spatial subharmonics. It is well known from the theory of nonlinear oscillations that the excitation of temporal subharmonics is usually a result of a nonlinear resonance between the frequency of the external force and the characteristic frequencies.<sup>17</sup> In this case, increasing the friction coefficient suppresses the subharmonic oscillations; therefore, in order to clarify the conditions for appearance of steady-state spatial subharmonics in the PRC, it is very important to investigate the character of the periodic motion of a particle subject to Eq. (10), in the absence of an external force and neglecting the dissipative parameter  $\nu_E$ . Replacing  $e \rightarrow x$ ,  $x' \rightarrow t$  in this section for clarity, we have from (10) that

$$\ddot{x} = -\partial U/\partial x, \quad U = \varepsilon(x - c \ln x). \quad (15)$$

Using (15) and the condition  $\bar{x} = 1$ , the constant  $c$  is easily related to the characteristic intensity of the oscillations, which is the average value of the squared velocity:

$$c = 1 - \varepsilon^{-1}\bar{x}^2. \quad (16)$$

Thus, the form of the potential  $U(x)$  is self-consistently related to  $\bar{x}^2$ . From the form of  $U(x)$  and Eq. (16), it follows that periodic motion is possible only for  $\varepsilon > 0$ ,  $0 < c < 1$ , and  $x > 0$ . In this case we have  $0 < \bar{x}^2 < \varepsilon$  (the positiveness of  $\varepsilon$  implies that the intensity grating runs along the external field and not opposite to it). The minimum of  $U(x)$  corresponds to the value

$$x_0 = c, \quad U_0 = \varepsilon c(1 - \ln c). \quad (17)$$

The dependence of the shape of the potential on the constant  $c$  is illustrated in Fig. 2. Note that as  $c \rightarrow 0$  (i.e., when  $\bar{x}^2 \rightarrow \varepsilon$ ), the potential  $U(x)$  reduces to a semilinear form, in which the particle's motion to the left is bounded by a vertical elastically reflecting wall, and to the right by an inclined plane  $\varepsilon x$ .

Let us write the law of conservation of energy for (15) as

$$\mathcal{E} = 1/2\dot{x}^2 + U(x) - U_0 = \text{const}. \quad (18)$$

The energy  $\mathcal{E}$  must be treated as independent of the integration constant  $c$ . In what follows, in place of the constants  $\mathcal{E}, c$  it will be convenient for us to use the equivalent set  $W, c$ , where  $W = \mathcal{E}/\varepsilon c$ .

Integrating (15), we find the oscillation period  $T_0(W, c)$  simply:

$$T_0 = 2\pi \left(\frac{c}{\varepsilon}\right)^{1/2} \Phi_0(W), \quad \Phi_0 = \frac{1}{2^{1/2}\pi} \int_{x_1}^{x_2} (W - U)^{-1/2} dx, \quad (19)$$

where  $\tilde{U} = x - 1 - \ln x$ , while  $x_{1,2}(W)$  are the turning points ( $x_2 > x_1$ ), determined by the equation  $\tilde{U} = W$ . In an analogous fashion, we find the average value of the coordinates

$$\bar{x} = \frac{2\pi}{T_0} \frac{c^{1/2}}{\varepsilon^{1/2}} \Phi_1(W), \quad \Phi_1 = \frac{1}{2^{1/2}\pi} \int_{x_1}^{x_2} (W - U)^{-1/2} x dx. \quad (20)$$

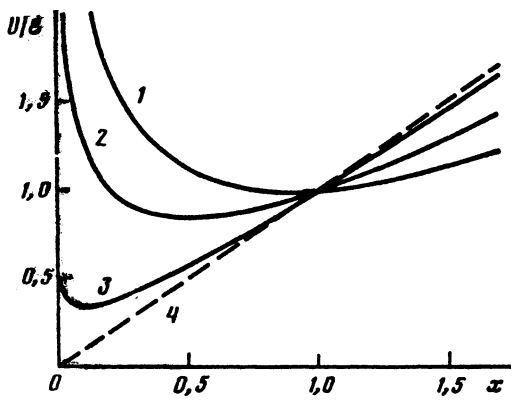


FIG. 2. Shape of the potential  $U(x)$  for different values of the constant  $c = 0.9$  (1),  $0.5$  (2),  $0.1$  (3). The ray  $U = \epsilon x$  (4) corresponds to the limit of the branches as  $c \rightarrow 0$ .

Using the conditions  $\bar{x} = 1$ , we obtain from (19), (20) the important relations

$$\frac{\bar{x}^2}{\epsilon} = 1 - \frac{\Phi_0(W)}{\Phi_1(W)}, \quad T_0 = \frac{2\pi \Phi_0^{1/2}(W)}{\epsilon^{1/2} \Phi_1^{1/2}(W)}. \quad (21)$$

The functions  $\Phi_{0,1}(W)$  are not difficult to find by numerical integration, and their asymptotic properties can be exhibited analytically: in particular,  $\Phi_{0,1} \rightarrow 1$  as  $W \rightarrow 0$ , while for  $W \rightarrow \infty$  we have  $\Phi_0/\Phi_1 \rightarrow 0$ ,  $\Phi_0^{3/2}/\Phi_1^{1/2} \rightarrow \sqrt{3}/\pi \approx 0.55$ . Taking (16) into account, we see that the case  $W \rightarrow 0$  corresponds to that of small harmonic oscillations:  $\bar{x}^2 \rightarrow 0$ ,  $c \rightarrow 1$ ,  $T_0 \rightarrow 2\pi/\sqrt{\epsilon}$ . For  $W \rightarrow \infty$  we have  $\bar{x}^2 \rightarrow \epsilon$ ,  $T_0 \rightarrow 2\sqrt{3}/\sqrt{\epsilon}$ ; this limit corresponds to motion in the semilinear potential ( $x_0 \rightarrow 0$ ,  $U_0 \rightarrow 0$ ).

The fact that Eq. (21) allows us to express the oscillation period  $T_0$  as a function of  $\epsilon$  and  $\bar{x}^2$  has important implications for understanding the physics. We may say that these variables specify the nonlinear shift in the frequency of the characteristic oscillations, i.e., the dependence of  $\omega_0 \equiv 2\pi/T_0$  on the characteristic intensity of the motion  $\bar{x}^2$  for fixed  $\epsilon$ . Of course, it is necessary to keep in mind that the association  $x(t)$  is, generally speaking, not harmonic. Therefore, not only the frequency  $\omega_0$ , but also the frequencies  $2\omega_0$ ,  $3\omega_0$ , etc. are present in its Fourier spectrum.

In our mechanical model, the periodic external force has unit frequency. Therefore, the condition for resonance with the characteristic oscillations has the form

$$n\omega_0 = 1, \quad n = 1, 2, 3 \dots \quad (22)$$

The case  $n = 1$  corresponds to ordinary (linear) resonance, the case  $n = 2$  to the  $1/2$  subharmonic,  $n = 3$  to the  $1/3$  subharmonic, etc. Nonlinear resonance can be viewed as decay of a pump quantum into  $n$  quanta of the characteristic oscillations. Combination nonlinear resonances are possible as well, corresponding to the condition  $n\omega_0 = n_1$  (Ref. 17).

Taking into account that the characteristic frequency  $\omega_0$  is a function of  $\epsilon$  and  $\bar{x}^2$ , we see that each of the resonance conditions (22) gives rise to a branch  $\bar{x}^2 = F_n(\epsilon)$ . It is noteworthy that all of these branches are similar: the function  $F_n(\epsilon)$  is obtained from  $F_1(\epsilon)$  by contracting the scales with respect to  $\bar{x}^2$  and  $\epsilon$  by a factor of  $n^2$ . It is easy to verify

this using Eq. (21). The branch  $F_n(\epsilon)$  taken as its origin the point  $\epsilon = 1/n^2$ ,  $\bar{x}^2 = 0$ , and terminates at the point  $\epsilon = \bar{x}^2 = 3/\pi^2 n^2$ . The first three branches are shown in Fig. 3. It is clear that the branch  $F_1(\epsilon)$ , which corresponds to linear resonance, is single-valued. However, for the subharmonic branches ( $n \geq 2$ ) there are both single-valued and multivalued intervals of  $\epsilon$ . For small  $\epsilon$  there is a crossing of the branches, and an increase in the multiple-valuedness of  $\bar{x}^2$ . The structure of the branches shown in Fig. 3 indicates unambiguously that a variety of hysteresis phenomena are possible as  $\epsilon$  increases and decreases.

From general considerations, we can expect that under the action of an external force  $\epsilon m \cos t$  these branches undergo splitting and distortion. For small values of the modulation coefficient  $m$ , these effects will necessarily be small. However, we may hope that the distortions will be weak even for  $m \approx 1$  due to the numerical smallness of  $\epsilon$ . The simplest treatment of the oscillating external force can be made in two situations—close to the origin of a branch, where the anharmonicity is weak, and near the end of a branch, where we can use the semilinear approximation for  $U(x)$ . The first case will be treated systematically in Sec. 4. With regard to the second case, we will limit ourselves to a brief comment. For  $n = 2$ , integration of the equations of motion shows splitting of less than 1% near the end of the branch. In this case, the amplitude of the subharmonic oscillations with frequency  $1/2$  is several times greater than  $e_1$ ; higher harmonics corresponding to frequencies  $3/2$ ,  $2$ , etc. are numerically small.

Inclusion of the attenuation associated with the discarded terms can cause the region in which the branches we have found to shrink. For sufficiently large values of the parameters  $\nu_{E,N,D}$  the subharmonic branches can disappear completely. It is obvious that the higher nonlinear resonances, i.e., higher subharmonics, will be the first to be suppressed. Clearly the influence of dissipation effects will be stronger near the ends of the branches, since the semilinear approximation for the potential corresponds to an abrupt change in the velocity of particles near the left-hand turning point.

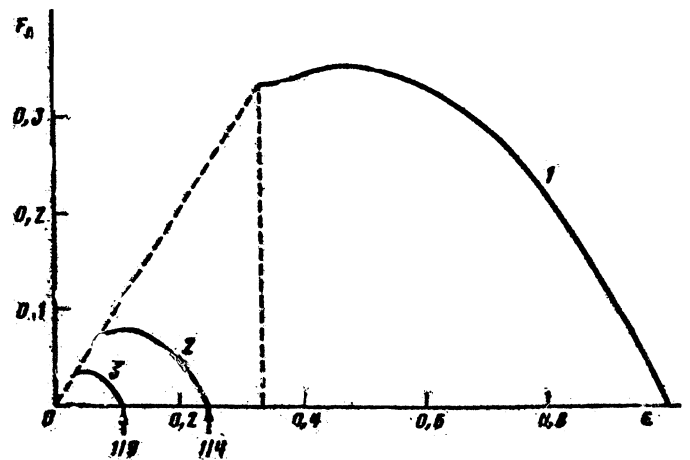


FIG. 3. The functions  $F_n(\epsilon)$  for  $n = 1, 2, 3$  (corresponding to curves 1, 2, 3), which correspond to linear resonance and the subharmonics  $1/2$  and  $1/3$ .

#### 4. STEADY-STATE SMALL-AMPLITUDE SUBHARMONICS

It follows from the mechanical analogy discussed in Sec. 3 that we should look for the 1/2 and 1/3 subharmonics, which have small amplitude, near the points  $\varepsilon = 1/4$  and  $\varepsilon = 1/9$ , respectively. In what follows, we will investigate the steady-state regime, based on perturbation theory with respect to the subharmonic amplitude. The theory we present is analogous in its content to the theory of nonlinear resonances.<sup>17,18</sup>

##### Subharmonic 1/2

Let us seek  $e(x')$  in the form

$$e - 1 = e_{1/2} \exp(ix'/2) + e_1 \exp(ix') + \text{c.c.} \quad (23)$$

Substituting (23) into the simplified equation (10) and isolating the spatial frequencies 1/2 and 1, we can readily obtain the following expression for  $e_{1/2}$  when  $|4\varepsilon - 1| \ll 1$ ,  $\nu_E \ll 1$  hold respectively:

$$|e_{1/2}|^2 = \frac{1}{5} (1/4 - \varepsilon) \pm \frac{1}{5} (m^2 - 36\nu_E^2)^{1/2}. \quad (24)$$

In accordance with our expectations we have two nearby branches of the solution; as  $\varepsilon$  decreases there is an increase in  $|e_{1/2}|$ . This increase obviously takes place from a value of zero.

Using perturbation theory with respect to the subharmonic amplitude, it is not difficult to take into account the influence of the terms that were discarded in going from the general system (7) to the simplified equation (10). Some uncomplicated calculations based on (7) show that Eq. (24) remains valid for  $\nu_{N,D} \ll 1$  if we replace  $\nu_E$  by  $\gamma_{1/2}$ , where

$$\gamma_{1/2} = \nu_E + \nu_N + \nu_D/4. \quad (25)$$

As follows from (24), the subharmonic 1/2 exists only for sufficiently small attenuation

$$6\gamma_{1/2} \leq m, \quad (26)$$

while as  $m \rightarrow 6\gamma_{1/2}$  the splitting of the branches reduces to zero. Setting  $|e_{1/2}|^2$  equal to zero, we obtain from (24) the limiting values  $\varepsilon_{\pm}$  given by

$$\varepsilon_{\pm} = \frac{1}{4} \pm \frac{1}{12} (m^2 - 36\gamma_{1/2}^2)^{1/2}. \quad (27)$$

These values characterize the threshold for the appearance of the subharmonic 1/2, and can be found from the condition that the system of equations be solvable with respect to  $e_{1/2}$  and  $e_{1/2}^*$ , without appealing to mechanical analogies.

As we will see in Sec. 5 below, the range  $\varepsilon_- < \varepsilon < \varepsilon_+$  corresponds to a temporal instability of the steady-state solution (12) with respect to the subharmonic 1/2. When  $m = 1$ ,  $\gamma_{1/2} = 0$  hold, Eq. (27) gives  $\varepsilon_+^{\max} = 1/3$ ,  $\varepsilon_-^{\min} = 1/6$ .

In view of the applicability conditions for the theory we have developed above, which is based on perturbation theory, we might expect that for  $m = 1$  the accuracy of Eqs. (24) and (27) will be rather poor. However, improving the perturbation theory by including the harmonic  $e_{3/2}$  and leading terms in the parameter  $\varepsilon = 1/4$  results only in corrections on the order of a few percent. Comparison with the results of numerical experiments also lead us to this conclusion. Thus, for  $m \approx 1$  the smallness of higher-order corrections to perturbation theory is ensured by the numerical parameters.

Using (24) it is easy to find the values of the derivative  $d(e_{1/2})^2/d\varepsilon$  for  $\varepsilon = 1/4$  and  $m, \gamma_{1/2} \rightarrow 0$ . This value, which equals  $-1.2$ , coincides to high accuracy with the initial slope of the curves in Fig. 3. Consequently, we obtain good agreement with the results based on our mechanical analogy. The relatively large extent of the initially linear segments of the branches shown in Fig. 3 attests to the very wide region of applicability of our perturbation theory expressions in the parameter  $\varepsilon$ . We also note that the smallness of  $e_{1/2}$  and  $e_1$  compare to unity guarantees the smallness of  $e_{3/2}$ . At the same time, it is possible to have  $e_{1/2} \gtrsim e_1$ .

##### Subharmonic 1/3

Let us seek  $e(x')$  in the form

$$e - 1 = e_{1/3} \exp(ix'/3) + e_{2/3} \exp(2ix'/3) + e_1 \exp(ix') + \text{c.c.} \quad (28)$$

Assuming  $\nu_E \ll 1$ ,  $\varepsilon \approx 1/9$ , we obtain from (10) the following system of equations

$$\begin{aligned} 2(1 - 9\varepsilon + 3i\nu_E)e_{1/3} + 10e_{1/3}^*e_{2/3} + 26e_1e_{2/3}^* &= me_{2/3}^*, \\ 6e_{2/3} + 2e_{1/3}^2 + 20e_1e_{1/3} &= me_{1/3}^*, \quad 16e_1 + 10e_{1/3}e_{2/3} = m. \end{aligned} \quad (29)$$

Taking into account the smallness of the amplitude, we have from this the following expressions for  $e_{1/3}$ ,  $e_{2/3}$ :

$$\begin{aligned} 1 - 9\varepsilon &= \frac{5m^2}{384} + \frac{5}{3}|e_{1/3}|^2 \pm \left[ \left( \frac{5m}{16} \right)^2 |e_{1/3}|^2 - 9\nu_E^2 \right]^{1/2}, \\ e_{1/3} &\approx -\frac{1}{3}(e_{1/3}^2 + \frac{1}{8}me_{1/3}^*). \end{aligned} \quad (30)$$

Inclusion of the diffusion of electrons and reoccupation of traps based on system (7) reduces to the replacement  $\nu_E \rightarrow \gamma_{1/3}$ , where

$$\gamma_{1/3} = \nu_E + \nu_N + \nu_D/9. \quad (31)$$

It follows from (30) that excitation of the subharmonic 1/3 is "hard"; i.e., the minimum possible value of  $|e_{1/3}|$  for fixed  $m$  and  $\gamma_{1/3}$  is nonzero:

$$|e_{1/3}|_{\min} = 48\gamma_{1/3}/5m, \quad (32)$$

which is reached for  $\varepsilon - 1/9 \approx -1.4 \cdot 10^{-3} m^2 - 17\gamma_{1/3}^2/m^2$ . Thus, in order to realize the solution we have found we require the condition  $\gamma_{1/3} \ll 0.1 m$ , which is more restrictive than the condition for excitation of subharmonic 1/2. The behavior of  $|e_{1/3}(\varepsilon)|$  for several values of the parameters  $m, \gamma_{1/3}$  is shown in Fig. 4.

As  $m \rightarrow 0$ ,  $\gamma_{1/3} \rightarrow 0$ , both values of  $|e_{1/3}|^2$  reduce to  $3(1 - 9\varepsilon)/5$ . This corresponds to  $(e_x^-)^2 \approx 2(1 - 9\varepsilon)/5$  and once more we find agreement with the initial slope of the branch shown in Fig. 3.

#### 5. STABILITY OF THE STEADY STATE WITHOUT SUBHARMONICS

Let us now investigate the temporal stability of the steady-state solutions found in Sec. 2. For simplicity we will start with the simplified system of equations (9).

Let us first consider stability against the 1/2 subharmonic. For this we write the system (9) in the form of a single higher-order equation for  $e(x', t')$ , substituting into it the expansion (23); we treat  $e_1$  as a constant quantity, and  $e_{1/2}(t')$  as a small perturbation. After separating out the spatial frequency 1/2 we are led to a linearized equation for

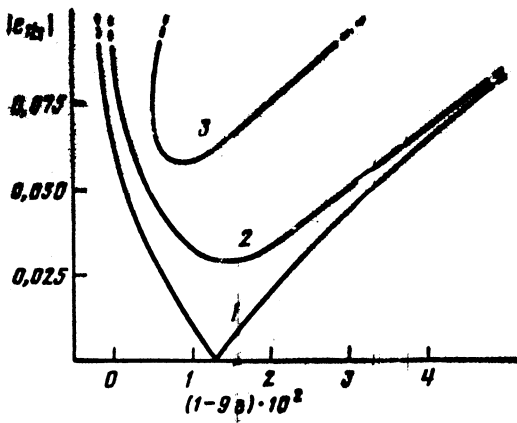


FIG. 4. The subharmonic branch  $|e_{1/3}(\varepsilon)|$  near  $\varepsilon = 1/9$ ; 1— $\gamma_{1/3} = 0$ ,  $m = 1$ ; 2— $\gamma_{1/3} = 0.003$ ,  $m = 1$ ; 3— $\gamma_{1/3} = 0.003$ ,  $m = 0.5$ .

the amplitudes  $e_{1/2}$  and  $e_{1/2}^*$ . Assuming these amplitudes are proportional to  $\exp(\Gamma t')$ , it is not difficult to obtain the following expression for the growth rate  $\Gamma$ :

$$\frac{\Gamma}{\Delta} = -v_E \pm 2 \left[ \left( \frac{m}{12} \right)^2 - \left( \varepsilon - \frac{1}{4} \right)^2 \right]^{1/2}. \quad (33)$$

The same assumptions are true with regard to  $v_E$  and  $\varepsilon$  as in Sec. 4. The instability can correspond only to the plus sign in Eq. (33).

It follows from (33) that instability occurs for  $\varepsilon_- < \varepsilon < \varepsilon_+$  where  $\varepsilon_{\pm}$  are the limiting values for the appearance of the small-amplitude steady-state 1/2 subharmonic solution given by Eq. (27). Within the interval under discussion we have  $\Gamma > 0$ ; at its edges  $\Gamma = 0$  holds, and beyond them  $\text{Re } \Gamma < 0$ . The maximum value of the growth rate  $\Gamma_{\text{max}} = \Delta(m/6 - v_E)$  is reached for  $\varepsilon = 1/4$ . For  $v_E > m/6$ , there is no instability for any  $\varepsilon$ . We can include the dissipative parameters  $v_D$  and  $v_N$  by making the replacement  $v_E \rightarrow \gamma_{1/2}$ . Thus, the disappearance of the instability is simultaneously accompanied by disappearance of the steady-state solution for  $e_{1/2}$ .

Starting from this analysis, we may expect that the upper branch  $|e_{1/2}(\varepsilon)|$ , which corresponds to the plus sign in (24), is stable, while the lower sign corresponds to instability. If this is the case, it is possible for two stable states to coexist for  $\varepsilon < \varepsilon_-$ , one containing the subharmonic 1/2, the other not.

Investigations of stability against creation of  $e_{1/3}$ ,  $e_{2/3}$  can be carried out analogously. The fundamental results reduce to the following: near  $\varepsilon = 1/9$  a steady-state solution without subharmonics is stable. This result should be expected in view of the harness of the branch  $e_{1/3}(\varepsilon)$ ; see Sec. 4. Actually, the fact that the real part of the growth rate reduced to zero ought to imply the existence of a 1/3 subharmonic solution with infinitely small amplitude. However, according to (32), the minimum value of  $|e_{1/3}|$  is finite. It is worth noting that a completely analogous situation occurs in the theory of nonlinear resonances.<sup>17,18</sup> If we pursue this analogy, we may expect that the smaller of the two values of  $|e_{1/3}|$  in Eq. (30) corresponds to the unstable segment of the branch.

In the general case, we should investigate stability by looking for perturbations  $ve$  in the form

$$\delta e = c_{\kappa} \exp(i\kappa x') + e_{1-\kappa} \exp[i(1-\kappa)x'] + \text{c.c.} \quad (34)$$

Doing so, we find that for  $\varepsilon \leq 1/4$  and sufficiently small  $v_{E,N,D}$  the perturbation is unstable for  $\kappa = (1 - \sqrt{1 - 4\varepsilon})/2$ . The growth rate  $\Gamma$  in this case is a complex quantity,  $\Gamma = \Gamma' + i\Gamma''$ , where

$$\frac{\Gamma'}{\Delta} = \frac{m\varepsilon^{1/2}}{1-\varepsilon}, \quad \frac{\Gamma''}{\Delta} = (1-4\varepsilon)^{1/2}. \quad (35)$$

The width of the region of instability  $\delta\kappa(\varepsilon)$  is rather small, increasing with increasing  $m$  and decreasing with increasing  $v_{E,N,D}$ . For  $\kappa = 1/3$ , the instability begins at  $\varepsilon = 2/9$ , while for  $\varepsilon = 1/9$  perturbations are amplified for  $\kappa \approx 0.13$ .

The nature of these instabilities is not difficult to understand once we realize that (7) implies the following circumstance: for  $m = 0$  and  $v_{E,N,D} \rightarrow 0$  a weakly attenuated bulk space-charge wave appears in the PRC with frequency  $\omega_{\kappa}$  and decay rate  $\gamma_{\kappa}$  where

$$\omega_{\kappa} = \frac{\varepsilon - \kappa^2}{\kappa}, \quad \gamma_{\kappa} = v_N + \varepsilon v_D + \frac{\varepsilon}{\kappa^2} v_E. \quad (36)$$

Then we may view the instability as a result of the decay of a spatially oscillating field of zero frequency,  $e_1 \exp(ix') + \text{c.c.}$ , into two eigenwaves which satisfy the nonlinear synchronism condition for a quadratic nonlinearity; i.e.,  $\omega_{\kappa} + \omega_{1-\kappa} = 0$ . We also note that the parameters  $\gamma_{1/2}$  and  $\gamma_{1/3}$  that we have used are the values of  $\gamma_{\kappa}$  for  $\kappa = 1/3$  and  $1/2$ .

In summing up our stability analysis we note that the subharmonic 1/2 occupies a special position, arising as it does from the linear instability with the maximum growth rate. We should expect that the upper branch  $e_{1/2}(\varepsilon)$  will be stable, at least for small amplitudes. As for the branches  $e_{1/3}$ ,  $e_{1/4}$ , ..., the analytic investigation we have presented here gives us no reason to expect stability. However, it also does not prove the contrary, i.e., that higher subharmonics correspond to hard excitation.

## 6. CONDITIONS FOR THE EXISTENCE OF SUBHARMONICS

Let us discuss the experimental consequences of the theory presented here. To do so, we express the fundamental dimensionless parameters  $\varepsilon$  and  $v_{E,N,D}$  of the theory in terms of the PRC characteristics and the physical quantities  $E_0$ ,  $\Omega$ ,  $K$ ,  $I_0$ . Using (11) and (14), we have

$$\begin{aligned} \varepsilon &= \frac{4\pi q}{\bar{\varepsilon} K \Omega E_0} \frac{\alpha I_0}{\hbar \omega} \propto \frac{I_0}{K \Omega E_0}, \\ v_E &= \frac{1}{K E_0 \mu \tau} \propto \frac{1}{K E_0}, \\ v_D &= \frac{K T}{q E_0} \propto \frac{K}{E_0}, \\ v_N &= \frac{N_D}{N_A} \frac{s_i I_0}{\Omega} \propto \frac{I_0}{\Omega}. \end{aligned} \quad (37)$$

It is clear that the light intensity and detuning enter into (37) only through the ratio  $I_0/\Omega$ . Therefore, in order to describe the subharmonics it is sufficient to use the three experimental parameters  $E_0$ ,  $K$ , and  $I_0/\Omega$  (the fact that large values of the modulation depth  $m$  favor subharmonic gener-

ation is completely understandable and will not be discussed here).

Let us note the useful identity  $\varepsilon = \nu_E / \Omega t_d$ , which follows from Eq. (37); here  $t_d$  is the dielectric relaxation time, which is easily measured in the experiment. This identity implies that for the first subharmonic the detuning  $\Omega$  cannot exceed  $t_d^{-1}$ . In addition, it is useful for estimating  $\nu_E$  in terms of the experimental data.

It is important that the microscopic characteristics of the crystal only enter into (37) in the form of two combinations. Typical values of the product  $\mu\tau$  are known for the most important PRC (see Table I). the combination  $N_D s_i / N_A \approx \alpha / \hbar \omega N_A$  is known with less accuracy; however, information on it can also be found in the literature.<sup>2,4</sup> For BSO we will use the following parameters taken from Refs. 22 and 23:

$$\bar{\varepsilon} = 56, \quad \alpha = 1 - 2 \text{ cm}^{-1}, \quad N_D / N_A = 10^3, \\ \mu\tau = (0.4 \div 1) \cdot 10^{-6} \text{ cm}^2 / \text{V}, \quad N_A = 10^{16} \text{ cm}^{-3}.$$

The simplest necessary condition for the existence of subharmonics can be obtained even from the inequality  $\nu_E \lesssim 10^{-1}$ . Taking into account that the maximum value of  $K$  is comparable to  $2\pi/\lambda$ , where  $\lambda$  is the wavelength of the light, while  $E_0$  can only barely exceed  $10^5$  V/cm due to breakdown, we obtain  $\mu\tau \gg 10^{-9} \text{ cm}^2 / \text{V}$ .

For BSO, this condition is quite well fulfilled. However, according to Table I, crystals such as LiNbO<sub>3</sub>, LiTaO<sub>3</sub>, BaTiO<sub>3</sub> are not promising candidates for observing subharmonics.

In general, each subharmonic corresponds to a three-dimensional region in the parameter space  $K$ ,  $E_0$ , and  $I_0/\Omega$ . The size and shape of this region depends on the crystal characteristics (and the modulation depth  $m$ ). For unfavorable characteristics the region may disappear. We should regard the relations  $\gamma_{1/2} < 1/6$ ,  $\varepsilon = 1/4$  as sufficient conditions for the existence of the 1/2 subharmonic. Expressing  $I_0/\Omega$  in terms of  $\varepsilon$  and  $KE_0$  using (37), we can write these relations in the form of restrictions on  $K$  and  $E_0$ . When these restrictions are obeyed, the thickness of the region of existence of the 1/2 subharmonic with respect to the parameter  $I_0/\Omega$  is finite. Figure 5 demonstrates the restriction for  $K$  and  $E_0$  in BSO. It is clear that as  $\mu\tau$  decreases, the region of existence contracts and shifts in the direction of large  $E_0$  and small  $K$ . When the condition

$$9\bar{\varepsilon}/\pi q N_A > \mu\tau \quad (38)$$

is fulfilled, this region disappears entirely. For the value of  $N_A$  chosen here, the critical value of  $\mu\tau$  comes to roughly  $1.1 \cdot 10^{-7} \text{ cm}^2 / \text{V}^{-1}$ . In an analogous fashion, using the relations  $\varepsilon = 1/9$ ,  $\gamma_{1/3} \lesssim 0.03$  (see Sec. 4), we may investigate the conditions for existence of a steady-state 1/3 subharmonic.

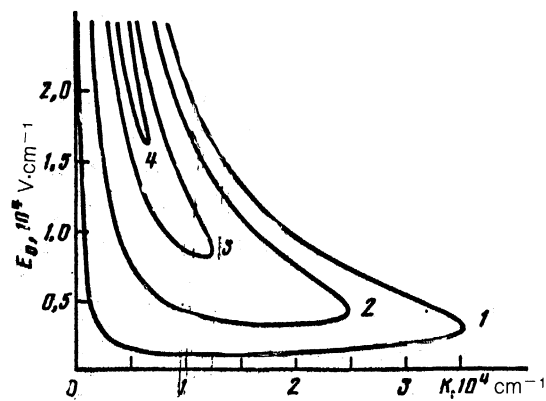


FIG. 5. Existence region of 1/2 subharmonic for  $T = 293$  K,  $m = 1$ , and various values of the parameter  $\mu\tau$ . Curves 1, 2, 3, and 4 are bounded by the regions corresponding to  $\mu\tau = 10 \cdot 10^{-7}$ ,  $2 \cdot 10^{-7}$ ,  $1.25 \cdot 10^{-7}$ , and  $1.15 \cdot 10^{-7} \text{ cm}^2 / \text{V}$ .

monic. In this case, the restriction on  $\mu\tau$  is much more stringent,  $\mu\tau \gtrsim 10^{-6} \text{ cm}^2 / \text{V}^{-1}$ . The shape of the allowed region in the  $K, E_0$  plane is similar to what is shown in Fig. 5.

Let us now consider restrictions on the parameters  $K$ ,  $I_0/\Omega$  at constant  $E_0$ . For this we make use of Eq. (27), which determines the limits of the region of instability against generation of the 1/2 subharmonic. The value of  $\gamma_{1/2}$  in this expression must be calculated at the resonance point, i.e., for  $\varepsilon = 1/4$ . From (27) and (37) it is completely obvious that for  $6\gamma_{1/2} \ll m$ , the permitted values of  $K$ ,  $I_0/\Omega$  are bounded by two nearby rays which leave the coordinate origin. However, for sufficiently small and sufficiently large values of  $K$ , the condition that  $\gamma_{1/2}$  be negligible ceases to be fulfilled. Because of this, the rays bend and close up. As  $\mu\tau$  (or  $m$ ) decreases, the region of permitted values shrinks and disappears. Typical results of analytical calculations are also shown in Fig. 6. To an accuracy of (5–10%) they coincide with the results of direct numerical modeling. Figures 5 and 6 are connected by a simple relation. If we extend the horizontal line  $E_0 = 8 \text{ kV/cm}$  in Fig. 5, the points where it intersects the curves that bound the region of existence of the 1/2 subharmonic (for fixed values of  $\mu\tau$ ) will correspond to the minimum and maximum values of  $K$  in Fig. 6.

Note that the 1/2 subharmonic can exist in the region of linear stability of the unperturbed solution for  $\varepsilon < \varepsilon_-$  as well. Therefore the region of existence of the 1/2 subharmonic can in practice be somewhat wider than what is shown in Fig. 6.

If the characteristics of the crystal are such that the parameters  $K$ ,  $E_0$ ,  $I_0/\Omega$  lead to an attenuation  $\gamma$  that is negligibly small, we can use scaling relations to describe the

TABLE I. Typical values of  $\mu\tau$  for several photorefractive crystals.

Crystal	$\mu\tau, \text{ cm}^2 \text{ V}^{-1}$	Crystal	$\mu\tau, \text{ cm}^2 \text{ V}^{-1}$
LiNbO <sub>3</sub>	$10^{-11} - 10^{-13}$	NBN	$10^{-9}$
LiTaO <sub>3</sub>	$10^{-12}$	BSO	$10^{-6} - 10^{-7}$
KNbO <sub>3</sub>	$10^{-8} - 10^{-11}$	BGO	$10^{-7}$
BaTiO <sub>3</sub>	$10^{-9} - 10^{-11}$	GaAs	$10^{-5} - 10^{-6}$

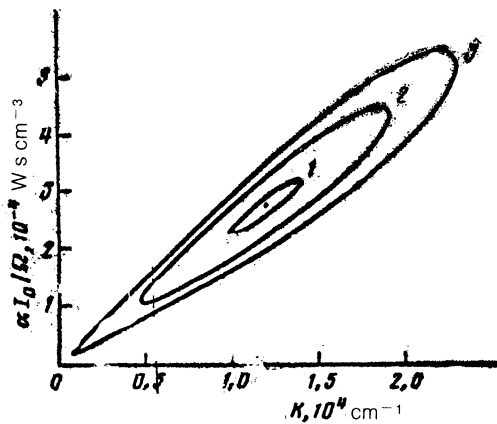


FIG. 6. Region of instability against the 1/2 subharmonic for  $E_0 = 8$  kV/cm and various values of  $\mu\tau$ . Curves 1, 2, and 3 correspond to  $\mu\tau = 2 \cdot 10^{-7}$ ,  $5 \cdot 10^{-7}$ , and  $10 \cdot 10^{-7}$  cm<sup>2</sup>/V. The dots indicate the limits of the region for  $\mu\tau \approx 1.26 \cdot 10^{-7}$  cm<sup>2</sup>/V.

steady-state properties of the subharmonics. These derive from the fact that the invariant steady-state characteristics require only constancy of the quantity  $K\Omega E_0/\alpha I_0$ .

It follows from expression (37) for  $\varepsilon$  that knowledge of the experimental parameters  $\alpha$ ,  $I_0$ ,  $E_0$ ,  $K$ , and  $\lambda$  allows us to calculate the threshold detuning value  $\Omega$ . In this case, however, it is necessary to keep in mind that the model we are investigating does not take into account the possibility of passive channels for optical absorption, which do not lead to the generation of free carriers. In order to include this possibility we must make the replacement  $\alpha \rightarrow \chi\alpha$ , where  $\chi$  is the quantum yield.

In concluding this section, let us discuss comparison with experiment. With regard to the first experimental paper (Ref. 8), the absence of quantitative data in this paper on  $\alpha$ , and  $\Omega$ , along with the fixed values of  $K$  and  $I_0$ , allow us to make only crude qualitative comparisons. The detunings coincide in order of magnitude. In accordance with the theory, there was an increase in the subharmonic index as  $\Omega$  increased. References 10–12 contain more quantitative data, including the dependence of the subharmonic  $e_{1/2}$  on  $E_0$ ,  $\Omega$ , and  $I_0$ . In accordance with theory the detuning  $\Omega$  necessary for excitation increased as the intensity  $I_0$  increased and decreased as  $E_0$  increased. Also in agreement with theory was the decrease in the subharmonic amplitude as its index  $n$  increased, and as the modulation depth  $m$  decreased. The quantitative data of Ref. 12 allow us to verify the predictions of the theory regarding the dependence of the subharmonic characteristics on the ratio  $I_0/\Omega$ . For values of the intensity  $I_0 = 1.75, 3.5, 5,$  and  $7$  mW/cm<sup>2</sup> this ratio (calculated at the maximum  $E_{1/2}(\Omega)$ ) was found to be 1, 1.2, 1, and 0.8 in arbitrary units. It is obvious that agreement with theory, which predicts constancy of this ratio, is satisfactory.

The possibility of detailed quantitative comparison between theory and experiment is hindered by the following circumstance. In Refs. 9–12 crystals were used with thickness  $l = 1$  cm. The value of the absorption coefficient  $\alpha$  was not given. However, it follows from data in the literature<sup>22,23</sup> that for BSO typical values of  $\alpha$  are  $(1-2)$  cm<sup>-1</sup> when  $\lambda = 514$  nm. Consequently, the ratio  $I_0/\Omega$  on which the subharmonic excitation depends changes significantly within

the crystal, and the quantitative experimental data are un-averaged.

Despite these difficulties, we will carry out a quantitative estimate of the optimum frequency detuning for the 1/2 subharmonic and compare it with experiment. Assuming  $\varepsilon = 0.2$ ,  $\alpha = (1-2)$  cm<sup>-1</sup>, taking into account that  $\chi$  ( $\lambda = 514$  nm)  $\approx 0.7$  (Ref. 24), and using the experimental parameters from Ref. 11, we find from (37) that  $\Omega = (9-12.5)$  sec<sup>-1</sup>. The experimental value is  $\Omega \approx (11-12)$  sec<sup>-1</sup>.

## 7. NUMERICAL MODELING

We carried out direct numerical modeling of the system of equations (7) with periodic boundary conditions on the segment  $s\Lambda$ , where  $\Lambda = 2\pi/K$  is the period of the fundamental grating, and  $s$  is an integer ( $1 \leq s \leq 12$ ). For  $s = 1$  we were able to investigate the solution without subharmonics, while in the remaining cases we studied the harmonics  $e_{1/2}, \dots, e_{1/12}$ . Knowing the solution without subharmonics allowed us to investigate its temporal stability with respect to period multiplication. Numerical noise served to initialize the subharmonics. Fourier analysis of the solution  $e(x, t)$  allowed us to track all the spatial harmonics of interest. The values of the coefficients in the modeled system (7) corresponded to the parameters of BSO chosen in Sec. 6.

Figure 7 shows the steady-state function  $|e_1(\varepsilon)|^2$  for solutions without subharmonics. The dashed curves correspond to the expressions from Sec. 2. It is clear that for  $\varepsilon \lesssim 0.3$  the agreement is good between the analytic and numerical results even for  $m \approx 1$ . As  $\varepsilon$  increases the role of the higher harmonics grows. Near a certain critical value of  $\varepsilon$ , which depends on  $m$ , a bifurcation of the solution occurs without subharmonics accompanied by hysteresis. This bifurcation obviously corresponds to a transition from the branch of forced "oscillations" to the branch of intrinsic nonlinear "oscillations" obtained earlier from the mechanical analogy (curve 1 in Fig. 3).

Figure 8 shows the dependence of the steady-state amplitudes  $e_{1/2}$  and  $e_1$  (obtained from temporal evolution of the numerical solutions) on the nonlinear parameter  $\varepsilon$ . The calculations were carried out on the interval  $12\Lambda$ , i.e., under conditions in which higher subharmonics  $e_{1/3}, e_{1/4}, \dots$  were allowed. In steady state these subharmonics were absent for the values of the crystal parameters chosen. As is clear from the figure, by allowing the numerical solution to evolve tem-

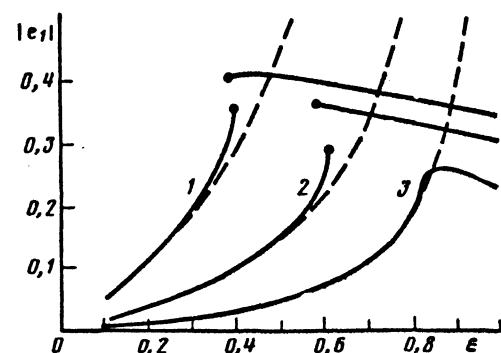


FIG. 7. Comparison of numerical and analytical results for the solutions without subharmonics: 1— $m = 0.9$ , 2— $m = 0.3$ , 3— $m = 0.1$ .

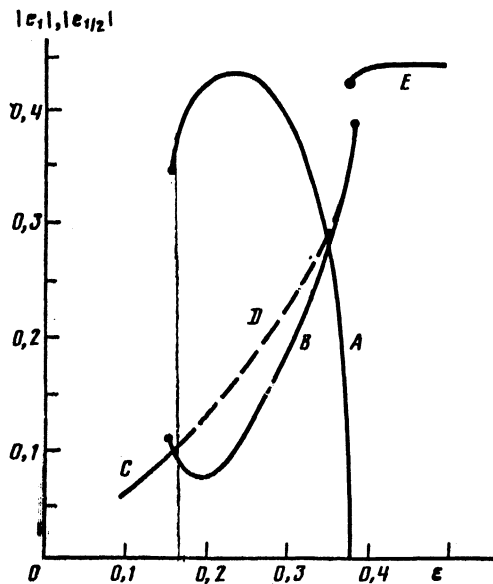


FIG. 8. Structure of 1/2 subharmonic branch for  $m = 1$ . Branch *A* corresponds to the 1/2 subharmonic, branch *B* to the fundamental  $e_1$  in the presence of  $e_{1/2}$ . The segments *C* and *D* of the branch correspond to the harmonic  $e_1$  in the absence of subharmonics, while segment *D* is unstable. Branch *E* is associated with the bifurcation of the solution without subharmonics.

porally we obtain a solution similar to the 1/2 subharmonic branch obtained from the mechanical analogy (Curve 2 in Fig. 3). From the data shown in Fig. 8, it follows that the smaller value of  $|e_{1/2}|$  in Eq. (24) corresponds to instability of the steady state, while the larger value corresponds to the steady-state segment of the branch. In agreement with the mechanical analogy (Sec. 3), near the end of the branch the harmonics  $e_{1/2}$  and  $e_{3/2}$  are not small compared to  $e_1$ . We note that the branch 1/2 found numerically ends at a somewhat larger value of  $\epsilon$  than is predicted by the mechanical analogy. This is obviously related to inclusion of the dissipative parameters  $\nu_{E,N,D}$ .

Changing the sign of the detuning  $\Omega$ , in agreement with the results of the analytic investigations (Sec. 3), causes the subharmonic regime to disappear.

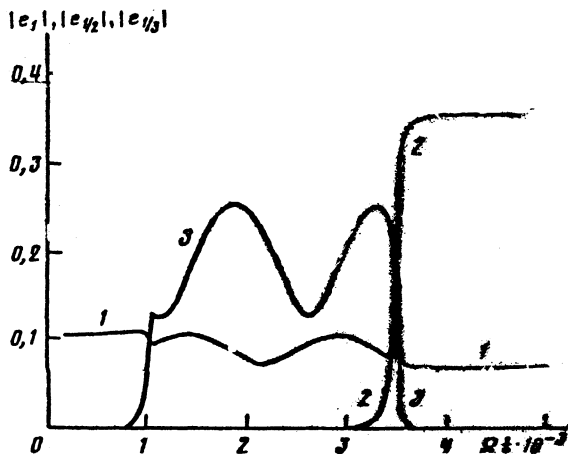


FIG. 9. Transient processes for 1/2 subharmonic: 1— $|e_1|$ , 2— $|e_{1/2}|$ , 3— $|e_{1/3}|$ .

The process of establishing the steady-state solutions described above is extremely nontrivial. At the intermediate stage, in addition to the fundamental harmonics and spatial frequencies of order 1/2, the 1/3 subharmonic is present as well, as is shown in Fig. 9, and is not small. It is a common feature of all the solutions that at least two characteristic times are present in the subharmonic temporal evolution. The rapidly varying time can be associated with the time constant  $t \sim \Omega^{-1} \epsilon^{-3/2}$ , which corresponds to Eqs. (33) and (35) for the growth rate  $\Gamma$ . The slower variation is obviously connected with terms of higher order in the original system (7).

We observed the steady-state 1/3 subharmonic in a very narrow region of experimental parameters (corresponding to  $\epsilon < 1/9$ ) for larger values of  $\mu\tau$ . Further investigations are required to determine the region of stability of this subharmonic.

## CONCLUSIONS

Let us summarize the basic results of this paper. Starting from constitutive equations that are standard for PRC, we have shown that solutions with the period of the external force  $\Lambda = 2\pi/K$  can be unstable against perturbations with new spatial frequencies, and in particular against the subharmonics 1/2 and 1/3. We have found criteria for the instability, and have investigated the fundamental subharmonic branches. Direct numerical modeling shows the establishment of a steady-state regime for the 1/2 subharmonic. The results we obtain explain the fundamental observed regularities, and give predictions for experiment. The simplest prediction is disappearance of the subharmonics when the frequency detuning or the external field changes sign.

It follows from our investigations that it would be very interesting to study experiments with thin crystals of BSO in the region of Bragg diffraction. Such experiments would allow us to identify the effects of instability of the constitutive equations on the effects of optical nonlinearities, and give nonaveraged results. Also promising would be investigations of subharmonics in semiconducting PRC with large values of the produce  $\mu\tau$ , e.g., in GaAs.<sup>25</sup>

We submit that the observed instability against creation of weakly attenuated space charge waves can lead not only to subharmonic steady-state solutions, but also to more complicated regimes, including temporal oscillations, three-dimensional structures, and chaos.

<sup>1)</sup> Temporal subharmonics are well known in the study of mechanical oscillatory systems;<sup>17,18</sup> sometimes they are also encountered in distributed systems as well.<sup>19</sup>

<sup>2)</sup> Our use of dimensionless variables is an unnatural way to treat space charge waves, which contain the parameters  $K$  and  $\Omega$ , since the quantities  $\gamma_x t'$  and  $\omega_x t'$  are actually independent of these quantities.

<sup>1)</sup> V. L. Vinetskii, N. V. Kukhtarev, S. G. Odoulov, and M. S. Soskin, *Usp. Fiz. Nauk* **129**, 113 (1979) [*Sov. Phys. Usp.* **22**, 742 (1979)].

<sup>2)</sup> P. Günter, *Phys. Rep.* **9**, 199 (1982).

<sup>3)</sup> B. Ya. Zel'dovich, N. F. Pilipetskii, and V. V. Shkunov, *Phase Conjugation* (in Russian), Nauka, Moscow, 1985.

<sup>4)</sup> Topics in Appl. Phys. **62**, **63**. *Photorefractive Materials* (Springer-Verlag, Berlin-Heidelberg, 1988, 1989).

<sup>5)</sup> B. I. Struman and V. M. Fridkin, *The Photogalvanic Effect in Crystals Without a Center of Inversion Symmetry, and Related Phenomena* (in Russian), Nauka, Moscow, 1992.

<sup>6)</sup> E. Ochoa, F. Vachas, and L. Hasselink, *J. Opt. Soc. Amer. A* **3**, 181 (1986).

<sup>7)</sup> R. Saxena and T. Y. Chang, *J. Opt. Soc. Amer. B* **9**, (1992).

<sup>8)</sup> S. Mallick, B. Imbert, H. Ducollet *et al.*, *J. Appl. Phys.* **63**, 5660 (1988).

- <sup>9</sup>D. C. Jones and L. Solymar, *Opt. Lett.* **14**, 743 (1989).
- <sup>10</sup>D. J. Webb, L. B. Au, D. C. Jones, and L. Solymar, *Appl. Phys. Lett.* **57**, 1602 (1990).
- <sup>11</sup>D. J. Webb and L. Solymar, *Opt. Comm.* **74**, 386 (1990).
- <sup>12</sup>J. Takacs and L. Solymar, *Opt. Lett.* (1992; in press).
- <sup>13</sup>K. H. Ringhofer and L. Solymar, *Appl. Phys. Lett. B* **53**, 1039 (1988).
- <sup>14</sup>K. H. Ringhofer and L. Solymar, *Appl. Phys. Lett. B* **48**, 395 (1989).
- <sup>15</sup>A. Novikov, S. Odoulov, R. Jungen, and T. Tshudi, *Opt. Lett.* **16**, 440 (1991).
- <sup>16</sup>L. B. Au, L. Solymar, and K. H. Ringhofer, Proc. Topical Conf. on "Photorefractive Materials, Effects, and Devices," Amiens, France, 1990.
- <sup>17</sup>L. D. Landau and I. M. Lifshits, *Mechanics* (3rd ed.), Pergamon, Oxford, 1973.
- <sup>18</sup>T. Hayashi, *Nonlinear Oscillations in Mechanical Systems* (Russian transl.), Mir, Moscow, 1968.
- <sup>19</sup>E. Schlömann, J. Green, and V. Milano, *J. Appl. Phys.* **61** (Suppl.), 386 (1960).
- <sup>20</sup>A. Blendovski, B. Sturman, J. Otten, and K. H. Ringhofer, Proc. Topical Conf. on "Photorefractive Materials, Effects, and Devices," Beverly, USA, 1991.
- <sup>21</sup>O. P. Nestiorkin, *Opt. Comm.* **81**, 315 (1991).
- <sup>22</sup>J. P. Herrian, D. Rojas, J. P. Huignard *et al.*, *Ferroelectrics* **75**, 271 (1987).
- <sup>23</sup>M. Peltrev and F. Micheron, *J. Appl. Phys.* **48**, 3683 (1977).
- <sup>24</sup>E. Sprague, *J. Appl. Phys.* **46**, 1673 (1975).
- <sup>25</sup>G. C. Valley, H. Rajbenbach, and A. J. von Bardenleben, *Appl. Phys. Lett.* **56**, 56 (1990).

Translated by Frank J. Crowne